

## Charge Redistribution and Transport in Molecular Contacts

Martina Corso,<sup>1,2,3,\*</sup> Martin Ondráček,<sup>4</sup> Christian Lotze,<sup>1</sup> Prokop Hapala,<sup>4</sup>

Katharina J. Franke,<sup>1</sup> Pavel Jelínek,<sup>4</sup> and J. Ignacio Pascual<sup>1,3,5</sup>

<sup>1</sup>*Institut für Experimentalphysik, Freie Universität Berlin, 14195 Berlin, Germany*

<sup>2</sup>*Centro de Fisica de Materiales CSIC/UPV-EHU, 20018 Donostia-San Sebastian, Spain*

<sup>3</sup>*Ikerbasque, Basque Foundation for Science, 48011 Bilbao, Spain*

<sup>4</sup>*Institute of Physics of the Academy of Sciences of the Czech Republic, 162 00 Prague, Czech Republic*

<sup>5</sup>*CIC nanoGUNE, 20018 Donostia-San Sebastian, Spain*

(Received 18 March 2015; revised manuscript received 8 July 2015; published 22 September 2015)

The forces between two single molecules brought into contact, and their connection with charge transport through the molecular junction, are studied here using non contact AFM, STM, and density functional theory simulations. A carbon monoxide molecule approaching an acetylene molecule ( $C_2H_2$ ) initially feels weak attractive electrostatic forces, partly arising from charge reorganization in the presence of molecular . We find that the molecular contact is chemically passive, and protects the electron tunneling barrier from collapsing, even in the limit of repulsive forces. However, we find subtle conductance and force variations at different contacting sites along the  $C_2H_2$  molecule attributed to a weak overlap of their respective frontier orbitals.

DOI: [10.1103/PhysRevLett.115.136101](https://doi.org/10.1103/PhysRevLett.115.136101)

PACS numbers: 68.37.Ps, 34.20.Gj, 73.63.Rt, 74.55.+v

The formation of an atomic-sized contact between two solids is an intriguing problem in physics [1]. Basic properties of nanoscale solids and composite materials, such as adhesion, friction, or electrical conductance, depend on the nature of their contacts at the atomic level. At proximity length scales comparable to the atomic dimensions and the electronic Fermi wavelength, the onset of electrical and a mechanical contact can be independently defined and may occur at different atomic separations [2]. For example, electronic transport through atomic contacts in metals is ballistic before the mechanical contact (i.e., bond equilibrium position) because the strong hybridization of localized atomic orbitals precedes the point of mechanical stability [3]. Atomic-scale contacts may also endow the system with new properties. In covalent contacts between semiconductors or molecular radicals, the hybridization of frontier orbitals may be accompanied by a strong redistribution of charges creating electrostatic barriers [4] or reducing the conductance of the contact [5,6].

In contrast, the contact between (close-shell) molecules is weak and stabilized by van der Waals interactions. Thus, it has a larger bond equilibrium distance, and the electrical conduction decreases due to smaller wave-function overlap [7]. The weak intermolecular forces are, however, highly sensitive to small changes of their surrounding electrostatic landscape and to structural rearrangements [7,8]. This is a key concept behind the electronic functionality of soft organic materials because charge hopping and electronic delocalization are determined by the overlap of the molecular orbitals [9].

In this Letter, we study the correlation of electrical transport and short-range forces during the formation of a

weak contact between two molecules using simultaneous force and current measurements in a scanning tunneling microscope. To create a robust molecular junction, we use carbon monoxide (CO) functionalized tips. These have shown to be stable at very short distances. Numerous studies resolved the chemical structure of adsorbed molecules with atomic and bond resolution [10–16] at the onset of Pauli repulsion forces. As counter electrode, we used an acetylene molecule ( $C_2H_2$ ) on a copper substrate. We find that weak attractive forces are enhanced by the formation of dipoles induced by the charge reorganization due to the proximity of the molecules. The interaction landscape is further correlated with the tunneling transmission of the junction. The two molecules behave as chemically passive spacers, with low transmission tunneling channels even when compressive forces are applied. However, contacting the acetylene at the C=C bond leads to relatively larger electrical transmission, confirming that electrical properties of organic systems are very sensitive to details on their structure.

We used a combined STM/non contact AFM based on a qPlus sensor design [17] operated in frequency modulation mode [18], at 5 K and in ultrahigh vacuum [19]. We measured frequency shift  $\Delta f(x, z)$  plots, and determined the corresponding vertical force  $F_z(x, z)$  in the pN range using the Sader and Jarvis method [20]. To provide quantitative values of forces and energies between the molecules, we removed the  $\Delta f(x, z)$  background due to long-range forces between the metal tip and sample [21] [see Supplemental Material [22]]. For simultaneous conductance measurements  $G(x, z)$ , a small bias of 80 mV was applied [22].

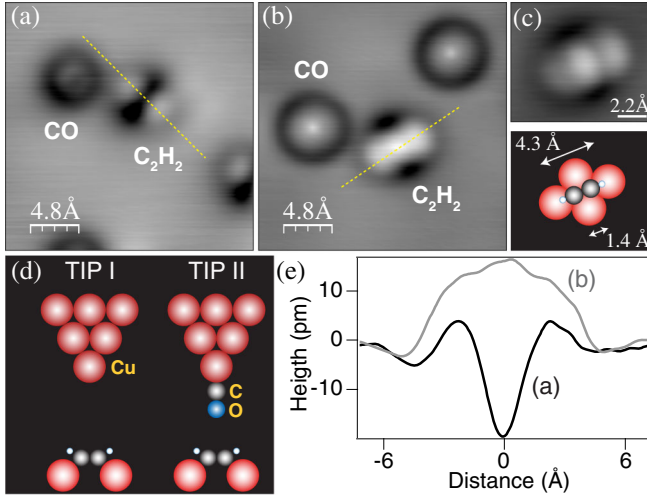


FIG. 1 (color online). (a), (b) Constant current STM images taken on CO and  $C_2H_2$  molecules in different sample positions at  $V = 100$  mV and  $I = 0.15$  nA. These images [(a) and (b)] were measured, respectively, with the tip terminations schematically drawn in (d): a sharp Cu tip (I) and a CO tip (II). The appearance of a  $C_2H_2$  with a CO tip and its adsorption geometry from [28] are shown in (c). (e) Topography profiles taken along the yellow lines measured on the  $C_2H_2$  in (a) and (b).

Acetylene molecules were deposited on a clean Cu(111) surface at 130 K, together with a small amount of CO molecules for functionalizing the tip apex. On the Cu(111) surface, acetylene undergoes a strong hybridization which converts the central  $sp$  bond into a double bond and bends the hydrogen atoms upwards [see Fig. 1(d)] [28]. We transferred a CO molecule to the apex of the STM tip as described in Ref. [29]. In most cases, the CO molecule adopts a standing up configuration on the tip apex, exposing the oxygen atom outwards [Fig. 1(d)] [30].

The shape of acetylene in the STM images varies depending on the termination of the tip apex. Figure 1 compares constant current STM images obtained with a sharp copper tip (a) and with a CO-functionalized tip (b) and (c). In the first case [Fig. 1(a)], acetylene is imaged with a characteristic dumbbell shape [31,32]. Using a CO functionalized tip, the contrast of acetylene is reversed, and appears with a three lobed structure peaked by a central maximum, clearly visible in the line profile in Fig. 1(e). This is due to the symmetry enhanced tunneling contribution from CO  $p$  orbitals into  $\pi^*$  states of acetylene [33].

*Electrostatic origin of short range forces.*—First, we address the identification of the interaction forces between CO and acetylene molecules in close proximity. Figure 2 shows the frequency shift ( $\Delta f$ ) and the integrated force as a function of their separation  $z$  [22]. Both molecules attract each other in a short distance range of  $\sim 2$  Å and form a stable bond at  $z = 0$  Å. We defined this point ( $z_0$ ) as the distance where short-range forces are relaxed [ $F_z(z_0)$ ], i.e., the energy minimum or equilibrium bond distance.

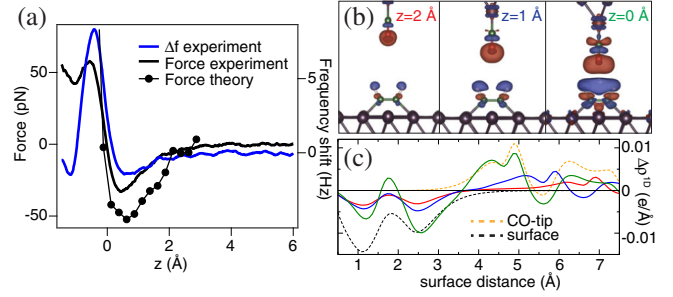


FIG. 2 (color online). (a) Frequency shift ( $\Delta f$ ) and the corresponding vertical force [20] measured with a CO functionalized tip at  $V = 0$  mV as a function of the tip-sample distance ( $z$ ) over the  $C=C$  bond of a  $C_2H_2$  molecule (further details in [22]).  $\Delta f$  is corrected for the macroscopic influence of the tip as explained in [22]. The calculated force is included as dots for comparison. (b) Development of the induced electron density  $\Delta\rho = \rho_{\text{tot}} - \rho_{\text{surf}} - \rho_{\text{tip}}$  and (c) its projection into  $z$ ,  $\Delta\rho^{1D} = \int \int \Delta\rho dx dy$  at three CO-acetylene distances. In (b), we plot  $\Delta\rho$  isosurfaces at  $0.0005 e/\text{\AA}$ , where blue and red mean depletion and accumulation of electrons, respectively. Dashed black and yellow lines in (c) show induced electron density of noninteracting free standing acetylene-surface and CO tip, when an electric field  $0.1 eV/\text{\AA}$  is applied.

The maximum attractive force before that point reaches  $33 \pm 5$  pN. The bond created between the two species is clearly noncovalent, with binding energy of  $-70 \pm 5$  meV [22].

Repulsive (Pauli) forces build up in the junction, when approaching the tip, to closer positions. In this region, a characteristic maxima in  $\Delta f$  can be observed, which gives rise to a small relaxation of forces at the junction [22]. As we shall show below, such relaxation can be attributed to the bending of the CO molecule at the tip.

To unveil the origin of the attractive molecular forces, we performed density functional theory (DFT)-based simulations of the interaction between the two molecules adsorbed in their respective environment (details are given in the Supplemental Material [22]). The force simulations reproduce well the results of the AFM measurement [Fig. 2(a)], obtaining a maximal attractive force of 52 pN over the center of the  $C_2H_2$  molecule. The force minimum is reached at a distance of 75 pm (50 pm in the experiment) before a relaxed bond is formed ( $F_z = 0$  point); thus, it is a short range force. This force has two main components. A fraction of it is due to molecular London dispersion forces, amounting to 27.5 pN. The rest is due to electrostatic forces related to static dipoles and to the charge redistribution induced by the proximity of the molecules.

The origin of this last attractive force component can be tracked down by analyzing the induced charge density ( $\Delta\rho$ ) due to the interaction between CO and  $C_2H_2$  molecules. Figure 2(b) shows  $\Delta\rho$  isosurfaces at three different CO- $C_2H_2$  separations, from the onset of attractive forces ( $z = 2$  Å) to the point of minimum energy,  $z_0$ . We observe,

in all the cases, no trace of electron accumulation in the CO-C<sub>2</sub>H<sub>2</sub> gap, supporting the absence of the covalent character of the bond between the two molecules. However, there is a growing charge redistribution as the molecules approach, leading to increasing polarization of the opposite sign of both CO and C<sub>2</sub>H<sub>2</sub>, and explaining the build up of attractive, short-range electrostatic forces.

The charge rearrangement in the absence of wavefunction overlap is due to the existence of a finite dipole moment of the molecules [34], and their effect on the local work functions of tip and sample: the CO molecule increases the copper work function, whereas C<sub>2</sub>H<sub>2</sub> decreases it [22]. The result is the existence of a finite electric field  $E_{10c}$  at the tunneling junction, which increases and enhances the electrical polarization of the molecules as they are approached. In fact, by applying a homogeneous electric field of  $E_z = 0.1$  eV/Å to either the CO-tip or C<sub>2</sub>H<sub>2</sub> sample, we obtain a similar charge redistribution as when the tip is at  $z_0$  [see dashed lines in  $\Delta\rho$  plots of Fig. 2(c)]. The electrostatic field  $E_{10c}$  built up at the junction causes variations of the local contact potential difference with the tip-sample separation, which are crucial for interpreting local Kelvin probe force spectroscopy measurements [4,35,36].

*Correlation of forces with charge transport.*—The absence of covalent character at the CO-C<sub>2</sub>H<sub>2</sub> bond implies that a tunneling mechanism may be required to describe the charge transport across the junction. Therefore, the electrical conductance is expected to be low but very sensitive to small forces affecting the molecular junction. To obtain the conductance of a relaxed CO-C<sub>2</sub>H<sub>2</sub> molecular junction, we measured, simultaneously, the linear conductance ( $G$ ) and  $\Delta f$  as a CO tip was approached at different sites along an acetylene molecule. The resulting  $G(x, z)$  and  $F_z(x, z)$  maps are shown in Fig. 3. The  $G(x, z)$  map corroborates that the conductance over the C=C bond of acetylene is the largest along the molecule [33,38]. The profile of bond equilibrium distance  $z_0(x)$  [white contour in Fig. 3(b)] shows a minimum at the C=C bond, reflecting that, at the center, forces have a shorter range (and are more attractive than over the H atoms [22]) probably due to the H atoms bending upwards. In the inset of Fig. 3(b), we plot the conductance values at the  $z_0(x)$  positions. The conductance of a CO molecule bonding to the C=C site of acetylene turns out to be a factor of 2 larger than when contacting the hydrogen atoms.

The measured tunneling conductance at the  $F_z(z_0) = 0$  turning point amounts to  $\sim 10^{-3}G_0$  ( $G_0 = e^2/\pi\hbar$ ) [Figs. 3(b) and 3(c)]. This low value confirms the persistence of a tunneling barrier at this contact point. In Fig. 4(a), we show the Hartree potential (the electrostatic potential felt by electrons) calculated in the gap between the CO at the tip and the C<sub>2</sub>H<sub>2</sub> molecule. The tunneling barrier does not collapse during the approach, and remains substantially above the Fermi level even when the force turning point  $z_0$  is reached and forces become repulsive. The calculated

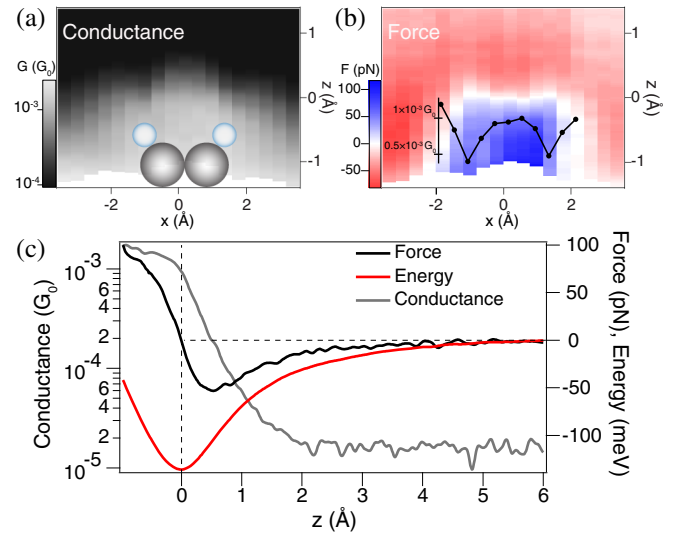


FIG. 3 (color online). (a), (b) Conductance and force maps recorded simultaneously along a C<sub>2</sub>H<sub>2</sub> molecular axis while applying a bias of  $V = 80$  mV to the sample. Similar force maps are obtained at zero bias [22]. The plot in (b) shows the value of the conductance at zero force.  $G$  is plotted in logarithmic scale in units of the quantum of conductance  $G_0 = 2e^2/h = (12906 \Omega)^{-1}$ . Both force and conductance are obtained after deconvolution of the tip oscillation [20,37]. (c) Conductance, force, and energy curves taken at the C=C bond with a CO tip. A change in conductance occurs at the energy minimum.

conductance is in all the process far below one quantum of conductance. This behavior is, thus, a characteristic of the noncovalent character of the bond, and contrasts with the case of metallic atomic contacts, where the tunneling barrier was found to collapse in contact [3], and the transport becomes ballistic.

*Bending of the CO molecule.*—Compressing the molecular junction into the repulsive regime leads to a change of slope in the  $G(z)$  plot [Fig. 3(c)] which resembles the transition to ballistic transport of metallic and molecular point contacts [39,40]. However, we note that this flattening coincides with an inflection also visible in the short-range  $F - z$  force curve, and is responsible for the characteristic peak observed in the  $\Delta f$  plots of Fig. 2(a) and in [22]. Thus, the flattening of the  $G(z)$  plot is a consequence of a mechanical rearrangement of the junction in order to relax repulsive forces [7]. The most probable change is the bending of the tip apex. It has been shown that a CO molecule on the apex can be easily tilted away from its original direction in response to lateral attractive forces [41,42]. In our case, sufficiently large repulsive forces in the junction (up to 50 pN, as seen in Fig. 2 and SOI) induce the lateral bending of the CO molecule [43] when approaching to potential saddle points such as the C=C bond. In this way, the CO molecule amplifies the response of the AFM to a potential landscape. This mechanism has been identified as responsible for intra-, and intermolecular bond contrast in constant height AFM images [44–47].

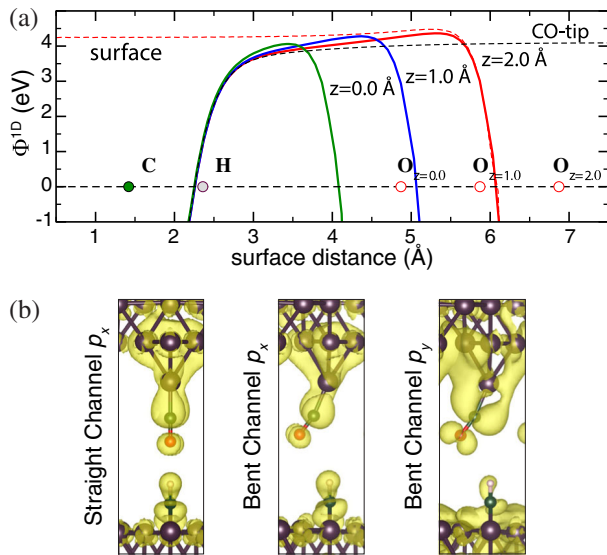


FIG. 4 (color online). (a) Development of the electrostatic (Hartree) potential felt by electrons in the gap between the tip and the acetylene molecule on the surface as the tip gradually approaches to the surface. The potentials are plotted along the CO molecular axis. Dashed black and red lines plot the electrostatic potential of the free standing surface and CO tip, respectively. The position of individual atoms of the acetylene molecule on the surface and oxygen atom on the tip at different tip-sample distances is schematically presented. All potentials are rendered with respect to the Fermi level. (b) Spatial distribution of the dominant eigenchannels at the Fermi energy for straight and bent CO configuration at the same tip-sample distance  $z = 0 \text{ \AA}$ .

The bending of the CO molecule affects the electron tunneling in two ways: First, it avoids the collapse of the tunneling barrier as the tip approaches. Second, it reduces the symmetry of the junction. To evaluate the impact of a reduced symmetry on tunneling, we calculated the transmission function of the different channels using nonequilibrium Green's function formalism implemented in the Smeagol code [48] together with the Fireball code [49]. Interestingly, the bending of the CO molecule over the C=C nodal plane leads to a swap of the leading transmission channels. For a straight CO tip, we find that the eigenchannel with  $p_x$  character is responsible for the majority of conductance ( $x$  direction along the C<sub>2</sub>H<sub>2</sub> axis), in agreement with [33]. The bending of the CO tip drastically reduces the transmission through this channel, while another channel with prevailing  $p_y$  orbital character dominates the tunneling. For a straight CO molecule, this channel was not active in the charge transport because its nodal plane lies along the C<sub>2</sub>H<sub>2</sub> axis. When the symmetry is reduced, one of its lobes couples with the C<sub>2</sub>H<sub>2</sub> orbitals [Fig. 4(c)], allowing the flow of charge (see Section S3 in the Supplemental Material [22]). The consequence of the tip bending is, thus, a change of symmetry of the main tunneling channel, which should lead to a change in conductance contrast for short distances.

In summary, the short range interactions between a small hydrocarbon such as acetylene and a CO molecule at the tip of an AFM show a weak attractive component originating from their intrinsic dipole moment and from the charge redistribution upon chemisorption. The electrical polarization of the molecules rises as they are brought into contact, leading to a gradual increase in the contact potential difference. However, the two molecules are chemically passive, and no chemical bond was formed even when they enter in a regime of repulsive forces. The lack of chemical activity protects the tunneling barrier from collapsing and allows us to perform stable force and conductance mapping in the regime of repulsive forces. We found that repulsive forces cause the bending of the CO molecule and the decrease of the stiffness of the junction.

We thank Peter Saalfrank for discussions. The research was supported by DFG (Grant No. Sfb 658), the Czech Science Foundation (GAČR) Project No. 14-02079S, GAAV Grant No. M100101207, and the Spanish MINECO (Grant No. MAT2013-46593-C6-01). M. C. acknowledges support from the Alexander von Humboldt Foundation.

\*Corresponding author.  
martina.corso@ehu.eus

- [1] N. Agrait, A. Levy-Yeyati, and J. M. van Ruitenbeek, *Phys. Rep.* **377**, 81 (2003).
- [2] U. Dürig, O. Züger, and D. W. Pohl, *Phys. Rev. Lett.* **65**, 349 (1990).
- [3] M. Ternes, C. González, C. P. Lutz, P. Hapala, F. J. Giesselbl, P. Jelínek, and A. J. Heinrich, *Phys. Rev. Lett.* **106**, 016802 (2011).
- [4] S. Sadewasser, P. Jelinek, C.-K. Fang, O. Custance, Y. Yamada, Y. Sugimoto, M. Abe, and S. Morita, *Phys. Rev. Lett.* **103**, 266103 (2009).
- [5] P. Jelínek, M. Svec, P. Pou, R. Perez, and V. Cháb, *Phys. Rev. Lett.* **101**, 176101 (2008).
- [6] A. Shiotari, Y. Kitaguchi, H. Okuyama, S. Hatta, and T. Aruga, *Phys. Rev. Lett.* **106**, 156104 (2011).
- [7] A. Yazdani, D. M. Eigler, and N. D. Lang, *Science* **272**, 1921 (1996).
- [8] N. Hauptmann, F. Mohn, L. Gross, G. Meyer, T. Frederiksen, and R. Berndt, *New J. Phys.* **14**, 073032 (2012).
- [9] V. Coropceanu, J. Cornil, D. A. da Silva Filho, Y. Olivier, R. Silbey, and J. L. Brédas, *Chem. Rev.* **107**, 926 (2007).
- [10] L. Gross, F. Mohn, N. Moll, P. Liljeroth, and G. Meyer, *Science* **325**, 1110 (2009).
- [11] L. Gross, F. Mohn, N. Moll, G. Meyer, R. Ebel, W. Abdel-Mageed, and M. Jaspars, *Nat. Chem.* **2**, 821 (2010).
- [12] F. Mohn, L. Gross, and G. Meyer, *Appl. Phys. Lett.* **99**, 053106 (2011).
- [13] G. Kichin, C. Weiss, C. Wagner, S. Tausz, and R. Temirov, *J. Am. Chem. Soc.* **133**, 16847 (2011).
- [14] N. Pavliček, B. Fleury, M. Neu, J. Niedenführ, C. Herranz-Lancho, M. Ruben, and J. Repp, *Phys. Rev. Lett.* **108**, 086101 (2012).

- [15] D. G. de Oteyza, P. Gorman, Y.-C. Chen, S. Wickenburg, A. Riss, D. J. Mowbray, G. Etkin, Z. Pedramrazi, H.-Z. Tsai, A. Rubio, M. F. Crommie, and F. R. Fischer, *Science* **340**, 1434 (2013).
- [16] A. Riss, S. Wickenburg, P. Gorman, L. Z. Tan, H.-Z. Tsai, D. G. de Oteyza, Y.-C. Chen, A. J. Bradley, M. M. Ugeda, G. Etkin, S. G. Louie, F. R. Fischer, and M. F. Crommie, *Nano Lett.* **14**, 2251 (2014).
- [17] F. J. Giessibl, *Appl. Phys. Lett.* **76**, 1470 (2000).
- [18] T. R. Albrecht, P. Grütter, D. Home, and D. Rugar, *J. Appl. Phys.* **69**, 668 (1991).
- [19] The qPlus sensor in this experiment is characterized by: a spring constant  $k_0 \approx 1.8$  kN/m, resonance frequency of  $f_0 = 20.7$  kHz, and quality factor  $Q \approx 1.6 \times 10^4$ . The data here presented are measured with a constant oscillation amplitude of  $A_{\text{osc}} \approx 30$  pm. The tip-sample distance is given as the vertical displacement from a reference position given by the set point parameters on the Cu substrate.
- [20] J. E. Sader and S. P. Jarvis, *Appl. Phys. Lett.* **84**, 1801 (2004).
- [21] Z. Sun, M. P. Boneschanscher, I. Swart, D. Vanmaekelbergh, and P. Liljeroth, *Phys. Rev. Lett.* **106**, 046104 (2011).
- [22] See Supplemental Material at <http://link.aps.org/supplemental/10.1103/PhysRevLett.115.136101> for details of the experimental and theoretical methods, the origin of short-range electrostatic interaction and an effect of the CO bending on the conductance, which includes Refs. [23–27].
- [23] G. Kresse and J. Furthmüller, *Phys. Rev. B* **54**, 11169 (1996).
- [24] D. Vanderbilt, *Phys. Rev. B* **41**, 7892 (1990).
- [25] J. P. Perdew, J. A. Chevary, S. H. Vosko, K. A. Jackson, M. R. Pederson, D. J. Singh, and C. Fiolhais, *Phys. Rev. B* **46**, 6671 (1992).
- [26] S. Grimme, *J. Comput. Chem.* **27**, 1787 (2006).
- [27] M. Paulsson and M. Brandbyge, *Phys. Rev. B* **76**, 115117 (2007).
- [28] W. Liu, J. S. Lian, and Q. Jiang, *J. Phys. Chem. C* **111**, 18189 (2007).
- [29] L. Bartels, G. Meyer, and K.-H. Rieder, *Appl. Phys. Lett.* **71**, 213 (1997).
- [30] S. Ishi, Y. Ohno, and B. Viswanathan, *Surf. Sci.* **161**, 349 (1985).
- [31] B. C. Stipe, M. A. Rezaei, and W. Ho, *Phys. Rev. Lett.* **81**, 1263 (1998).
- [32] Y. Konishi, Y. Sainoo, K. Kanazawa, S. Yoshida, A. Taninaka, O. Takeuchi, and H. Shigekawa, *Phys. Rev. B* **71**, 193410 (2005).
- [33] L. Gross, N. Moll, F. Mohn, A. Curioni, G. Meyer, F. Hanke, and M. Persson, *Phys. Rev. Lett.* **107**, 086101 (2011).
- [34] M. Schneiderbauer, M. Emmrich, A. J. Weymouth, and F. J. Giessibl, *Phys. Rev. Lett.* **112**, 166102 (2014).
- [35] F. Mohn, L. Gross, N. Moll, and G. Meyer, *Nat. Nanotechnol.* **7**, 227 (2012).
- [36] B. Schuler, S.-X. Liu, Y. Geng, S. Decurtins, G. Meyer, and L. Gross, *Nano Lett.* **14**, 3342 (2014).
- [37] J. E. Sader and Y. Sugimoto, *Appl. Phys. Lett.* **97**, 043502 (2010).
- [38] N. Pavliček, I. Swart, J. Niedenführ, G. Meyer, and J. Repp, *Phys. Rev. Lett.* **110**, 136101 (2013).
- [39] N. Néel, J. Kröger, L. Limot, T. Frederiksen, M. Brandbyge, and R. Berndt, *Phys. Rev. Lett.* **98**, 065502 (2007).
- [40] G. Schulze, K. J. Franke, A. Gagliardi, G. Romano, C. S. Lin, A. L. Rosa, T. A. Niehaus, Th. Frauenheim, A. Di Carlo, A. Pecchia, and J. I. Pascual, *Phys. Rev. Lett.* **100**, 136801 (2008).
- [41] M. Neu, N. Moll, L. Gross, G. Meyer, F. J. Giessibl, and J. Repp, *Phys. Rev. B* **89**, 205407 (2014).
- [42] A. J. Weymouth, T. Hofmann, and F. J. Giessibl, *Science* **343**, 1120 (2014).
- [43] From our DFT simulations, we obtain that the CO molecule undergoes the larger structural relaxation (165 pm lateral relaxation), whereas the relaxation of all acetylene atoms is less than 3 pm.
- [44] L. Gross, F. Mohn, N. Moll, B. Schuler, A. Criado, E. Guitián, D. Pea, A. Gourdon, and G. Meyer, *Science* **337**, 1326 (2012).
- [45] A. M. Sweetman, S. P. Jarvis, H. Sang, I. Lekkas, P. Rahe, Y. Wang, J. Wang, N. R. Champness, L. Kantorovich, and P. Moriarty, *Nat. Commun.* **5**, 3931 (2014).
- [46] P. Hapala, G. Kichin, C. Wagner, F. Stefan Tautz, R. Temirov, and P. Jelínek, *Phys. Rev. B* **90**, 085421 (2014).
- [47] S. K. Hämäläinen, N. van der Heijden, J. van der Lit, S. den Hartog, P. Liljeroth, and I. Swart, *Phys. Rev. Lett.* **113**, 186102 (2014).
- [48] A. R. Rocha, V. M. García-Suárez, S. Bailey, C. Lambert, J. Ferrer, and S. Sanvito, *Phys. Rev. B* **73**, 085414 (2006).
- [49] J. P. Lewis *et al.*, *Phys. Status Solidi B* **248**, 1989 (2011).